Space Sci Rev (2007) 130: 173–182
DOI 10.1007/s11214-007-9216-0

Isotopic Composition of the Solar Wind Inferred from In-Situ Spacecraft Measurements

R. Kallenbach · K. Bamert · M. Hilchenbach

Received: 11 February 2007 / Accepted: 10 May 2007 / Published online: 19 July 2007

Abstract The Sun is the largest reservoir of matter in the solar system, which formed 4.6 Gyr ago from the protosolar nebula. Data from space missions and theoretical models indicate that the solar wind carries a nearly unfractionated sample of heavy isotopes at energies of about 1 keV/amu from the Sun into interplanetary space. In anticipation of results from the Genesis mission's solar-wind implanted samples, we revisit solar wind isotopic abundance data from the high-resolution CELIAS/MTOF spectrometer on board SOHO. In particular, we evaluate the isotopic abundance ratios $^{15}N/^{14}N$, $^{17}O/^{16}O$, and $^{18}O/^{16}O$ in the solar wind, which are reference values for isotopic fractionation processes during the formation of terrestrial planets as well as for the Galactic chemical evolution. We also give isotopic abundance ratios for He, Ne, Ar, Mg, Si, Ca, and Fe measured in situ in the solar wind.

Keywords Isotopic composition · Solar system · Solar wind

1 Introduction

Solar system samples are usually compared to terrestrial material as a reference. However, because the Sun contains more than 99% of solar system matter, any non-nuclear fractionation process during the formation of the inner solar system from the early solar nebula could have changed the terrestrial isotopic composition, but not the solar isotopic composition. Consequently, solar matter is a better witness of the composition of the protosolar nebula than terrestrial material.

R. Kallenbach (✉) · M. Hilchenbach
Max Planck Institute for Solar System Research, Max-Planck-Strasse 2, 37191 Katlenburg-Lindau, Germany
e-mail: kallenbach@mps.mpg.de

R. Kallenbach · K. Bamert
Physikalisches Institut, University of Bern, Sidlerstrasse 5, 3012 Bern, Switzerland

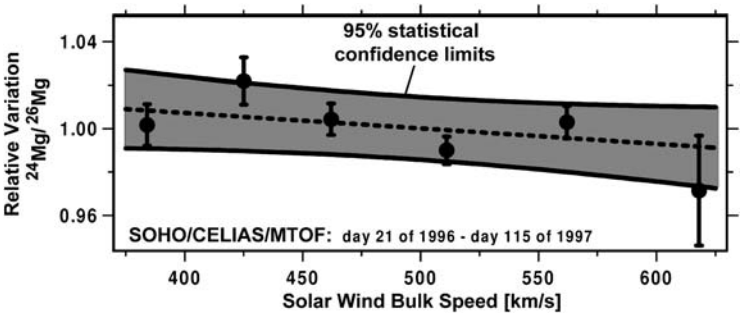

Fig. 1 Relative variation of the solar wind $^{24}Mg/^{26}Mg$ ratio versus the solar wind bulk speed. Data from Kallenbach et al. (1998a)

Kallenbach (2003) concluded from data of spaceborne instrumentation and from theoretical models that the solar wind carries a sample of heavy solar isotopes that is fractionated by, at most, about one percent per atomic mass unit (Fig. 1).

This review gives the most recent summary of solar wind isotopic abundance data from spaceborne sensors in order to give a reference for results soon to be expected from solar-wind implanted samples of the Genesis mission. The primary scientific objective of the Genesis mission is to determine the nitrogen and oxygen isotopic abundance ratio in the solar wind. These ratios are difficult to measure with spaceborne instrumentation, as will be discussed. Nonetheless, we give our best effort to constrain the values on the ratios $^{15}N/^{14}N$, $^{18}O/^{16}O$, and $^{17}O/^{16}O$ in the solar wind. These ratios are derived from data taken during the first two years of the SOHO mission. A more precise analysis may still be possible when evaluating all data of the SOHO mission which has operated for more than ten years.

2 Nitrogen Isotopes in the Solar System

The sources and reservoirs of nitrogen in the solar nebula from which planetary bodies formed are still under debate. The processes in the early solar nebula are usually understood in terms of the chemistry and physics of interstellar molecular clouds (Herbst 2003). Ion-molecule reactions at temperatures of 10–30 K enrich ^{15}N in the HCN and NH_3 molecules, while the dominant (>90%) form of nitrogen in interstellar clouds, molecular N_2, is relatively depleted in ^{15}N.

This overall picture matches qualitatively the measurements of the $^{15}N/^{14}N$ ratio in different solar system samples. The gas envelope of Jupiter presumably had been accreted from the volatile component of the solar nebula which mainly consisted of molecular N_2. The $^{15}N/^{14}N$ ratio of $(2.3 \pm 0.3) \times 10^{-3}$ in Jupiter's atmosphere (Owen et al. 2001; Abbas et al. 2004; Fouchet et al. 2004) is indeed lower than the $^{15}N/^{14}N$ ratio of $(3.10 \pm 0.45) \times 10^{-3}$ observed in HCN (Jewitt et al. 1997) in Comet Hale-Bopp (C/1995 O1). The CN radicals observed in comets de Vico (122P/1995 S1) and Ikeya-Zhang (153P/2002 C1) have even larger ^{15}N enrichments, $^{15}N/^{14}N \approx (6.5 \pm 2.0) \times 10^{-3}$ (Jehin et al. 2004). This points toward the existence of (an)other unknown parent(s) of CN besides HCN, with an even higher ^{15}N excess. These could be organic compounds like those found in interplanetary dust particles (Messenger et al. 2003).

Observations with the ion neutral mass spectrometer on board Cassini during the first flyby of Titan yield $^{15}N/^{14}N \approx (5.20 \pm 0.55) \times 10^{-3}$ in N_2 of Titan's atmosphere (Niemann et al. 2005), while the observations in HCN yield even higher ^{15}N, $^{15}N/^{14}N \approx 0.017$

(Lammer and Bauer 2003). Lammer and Bauer (2003) suggested that the ^{15}N enrichment in HCN indicates fractionation by gravitational escape from an early massive atmosphere, while Niemann et al. (2005) proposed that the ^{15}N enrichment in HCN relative to the ^{15}N in N_2 is caused by a photochemical process.

Most recently, Liang et al. (2007) measured the photoabsorption cross-section of NH_3 in the wavelength range 140 to 220 nm and concluded that NH_3 in Jupiter's atmosphere at the pressure level of 400 mbar, where the Galileo Probe measurements took place, should be depleted in ^{15}N with respect to nitrogen in the solar nebula. This leaves the solar wind as the only reliable witness for the protosolar isotopic composition of nitrogen.

The isotopic composition of nitrogen in the solar wind has been searched in lunar surface samples. Nitrogen that is implanted in the first tens of nanometers of lunar regolith grains and associated with the deuterium-free solar wind hydrogen is depleted in ^{15}N by at least 24% (Hashizume et al. 2000) with respect to nitrogen in the terrestrial atmosphere ($^{15}N/^{14}N \approx 0.00368$). In contrast, a component associated with deuterium-rich hydrogen in silicon-bearing coatings at the surface of ilmenite grains has been found to be enriched in ^{15}N with respect to terrestrial nitrogen. The strong enrichments in ^{15}N may be hard to explain with isotopic fractionation in only nebular or planetary environments. Possibly, the compounds strongly enriched in ^{15}N are of interstellar origin and never equilibrated in the protosolar nebula. These compounds may carry signatures of nucleosynthetic processes (Marty et al. 2003). About 90% of nitrogen in lunar regolith has been identified as non-solar (Wieler et al. 1999).

The measurement of the $^{15}N/^{14}N$ has been regarded as not feasible with the MTOF (mass time-of-flight) sensor of the Charge, Element, and Isotope Analysis System (CELIAS) onboard SOHO (Solar and Heliospheric Observatory). However, efforts have been made to retrieve the ^{15}N abundance in the solar wind by Kallenbach et al. (1998b), which we refer to as K98 hereafter. The main problems arise for principal instrumental reasons. In the spectra of the MTOF sensor, the $^{15}N^{+}$ counts have to be corrected for interference with $^{30}Si^{++}$, which has the same mass-to-charge ratio (Fig. 2). In K98, the $^{30}Si^{++}$ counts interfering with $^{15}N^{+}$ have been estimated from the $^{29}Si^{++}$ counts which are in principal isolated but hard to determine on top of the 'wing' of the $^{14}N^{+}$ & $^{28}Si^{++}$ main peak. In this reassessment, the $^{30}Si^{++}$ counts are estimated from the Si/N elemental abundance ratio which in turn is estimated from the Mg/O ratio. For Mg and Si the FIP (First-Ionization Potential) enrichment (von Steiger and Geiss 1989) over their photospheric abundance is approximately identical, while N and O are both high-FIP elements with very little FIP fractionation in the solar wind. During the measurement period for the data shown in Fig. 2 the FIP enrichment of Mg is approximately 1.4 (Kallenbach 2001) including instrumental fractionation. The MTOF sensor detects high-speed—that is, low-FIP-fractionation—solar wind more efficiently, which results in a lower count rate in the slow solar wind and a larger uncertainty for the high-FIP data in Fig. 3. In K98, a fit to the line shapes by analytical functions yielded a FIP enrichment of about 2.9. This value would match expectations of FIP fractionation in the slow solar wind. However, the elemental instrument efficiencies of the MTOF sensor have to be included for the analysis of the data in Fig. 2.

The discrepancy in the Si abundance implied by Kallenbach (2001) and that implied by K98 has motivated a more detailed analysis of the line shapes in the MTOF spectra, which is described in the Appendix for reproducability. The analysis using the current technique to describe the line shapes yields $^{14}N/^{15}N \approx 320$ or $^{15}N/^{14}N \approx (3.1 \pm 0.7) \times 10^{-3}$ (1σ-error). However, considering the uncertainty of the data analysis with such large background, we basically repeat the result of Kallenbach (2003) that $^{14}N/^{15}N > 200$ in the solar wind.

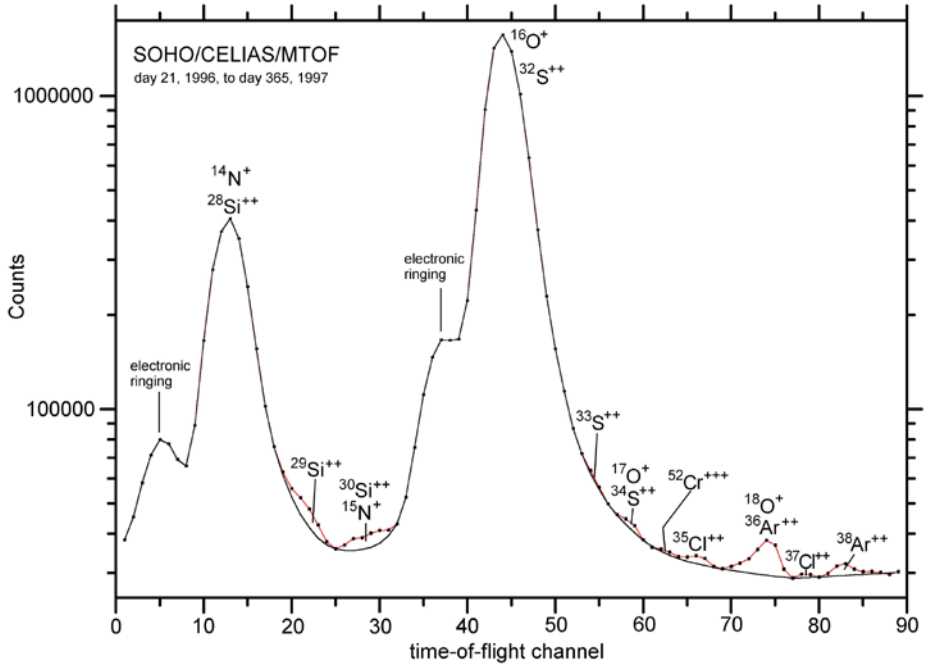

Fig. 2 The SOHO/CELIAS/MTOF spectrum in the atomic mass-per-charge range from about 13 to 20 for the time period 21 January 1996 to 31 December 1997. The data are identical to those published in Kallenbach et al. (1998b)

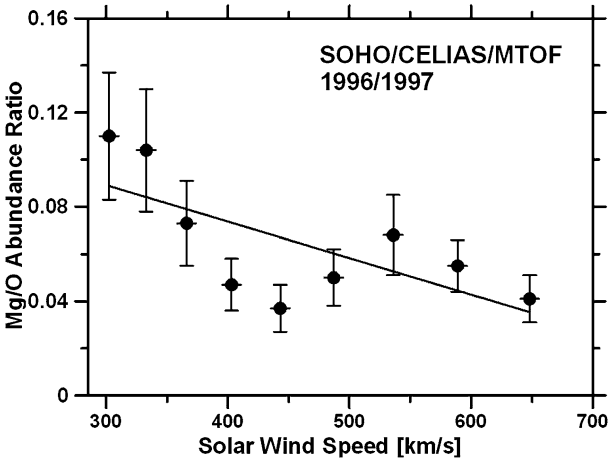

Fig. 3 The Mg/O ratio in the solar wind as measured with the MTOF sensor (Kallenbach 2001). The larger *error bars* at the high Mg/O ratio—that is, at high-FIP fractionation—are due to the lower detection efficiency of MTOF in the slow solar wind; that is, the count rates are lower in the slow solar wind

3 Oxygen Isotopic Ratios in the Solar System

Since the pioneering work of Thiemens and Heidenreich (1983), the process of photo-selfshielding is discussed in the context of isotopic ratios as tracers for planetary formation processes in the early solar nebula. The basic idea is that fractionation occurs through selective photo-dissociation of molecules such as $C^{17,18}O$, HD, or $^{14}N^{15}N$. The more abundant

molecules such as pure H_2, or $^{14}N_2$ or $C^{16}O$, absorb the respective ultraviolet (UV) line that dissociates them within a much smaller depth in the accretion disk. That means, the medium is optically thicker for these UV lines than for the shifted UV lines that are absorbed by the rare molecules. Therefore, relatively more $C^{17,18}O$ (HD, $^{14}N^{15}N$) molecules are dissociated so that relatively more $^{17,18}O$ (D, ^{15}N) radicals are available for chemical reactions. At present, a chemist divides the approximately cylindrical protoplanetary disk into three types of vertical layers: (1) the upper and lower photo-dissociation region (PDR), (2) the upper and lower molecular layer, and (3) the central condensation layer. The PDR is the outermost layer of the proto-planetary disk and is exposed to the UV, X-ray, and particle radiation of the young Sun, because the accretion disk is warped and becomes thicker at large distances from the Sun. The PDR is also exposed to radiation from the interstellar medium or from other stars. Closer to the central layer, molecules such as HCN or NH_3 are formed from the radicals. Oxygen may be incorporated into rocky and icy materials by the reactions (Clayton 2002)

$$\begin{aligned} Mg_{(g)} + SiO_{(g)} &\Rightarrow MgSiO_{3(s)} \\ H_{2(g)} + O_{(g)} &\Rightarrow H_2O_{(g)}. \end{aligned} \tag{1}$$

In the central condensation layer, molecules accrete on the surface of ices and dust grains. An important point of this view is that at almost any heliocentric distance the disk is exposed to optical and particle radiation from both the interstellar medium and the central star. Therefore, planetary material formed from ices and rocks that also have trapped HCN or NH_3 tends to be enriched in the rare isotopes with respect to solar material.

Recent work by Hashizume and Chaussidon (2005) indicates that the self-shielding of CO molecules is reflected in the oxygen isotopic ratios in lunar samples and the solar wind implanted into these samples (Fig. 4).

The data analysis for the MTOF data is again shown in the Appendix. We find $^{16}O/^{18}O \geq 500$. Although the ratio is rather uncertain it would be concordant with the conclusions of Hashizume and Chaussidon (2005). In a similar way, we find $^{16}O/^{17}O \geq 2000$ if there is no contribution of $^{34}S^{++}$ to the peak of $^{17}O^{+}$. However, this seems unlikely. Therefore, a depletion of ^{17}O in the solar wind with respect to terrestrial ^{17}O does not seem unlikely although it cannot be strongly supported by MTOF data because of the measurement's large uncertainty.

4 Summary

Table 1 summarizes the isotopic ratios measured in the solar wind by spacecraft instrumentation and compares these ratios to meteoritic values or to values determined with the Apollo Solar Wind Collection (SWC) Foil Experiment (Geiss et al. 1972).

Regarding the nitrogen and oxygen isotopic abundance ratios we can state only that the MTOF data do not deliver any contradiction to the results of Owen et al. (2001) and Hashizume and Chaussidon (2005) that the main isotopes ^{14}N and ^{16}O are enriched in the solar wind with respect to their abundance in terrestrial samples. This enrichment could indicate that the terrestrial isotopic composition of nitrogen and oxygen had been fractionated with respect to the main reservoir, the solar material, by the process of photo-selfshielding in the protosolar nebula. However, the MTOF data on the isotopic abundance ratios of oxygen and nitrogen in the solar wind are consistent with the terrestrial isotopic ratios as well.

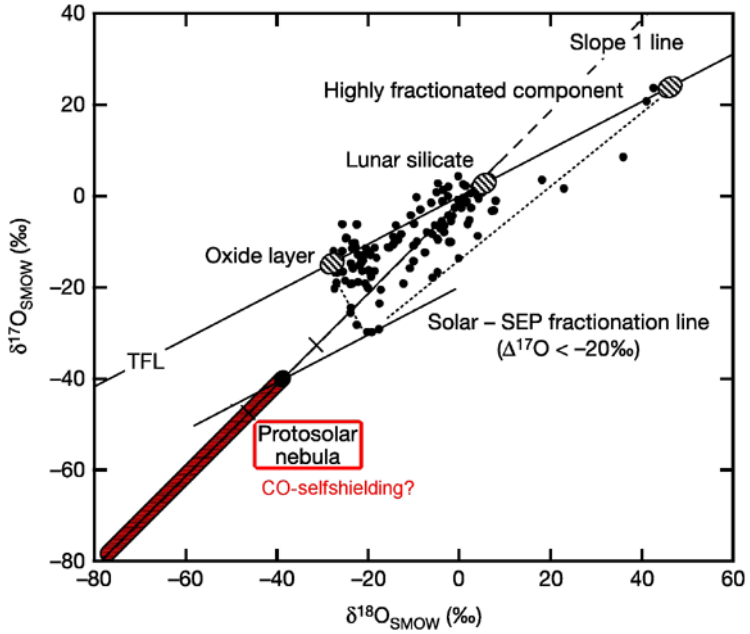

Fig. 4 Theoretical prediction of the solar-nebula fractionation line by Hashizume and Chaussidon (2005). The upper limit for the composition of the protosolar nebular gas is predicted to be $\delta^{17}O \approx \delta^{18}O = -4 \pm 0.8\%$ (1-σ error). The abbreviation TFL labels the terrestrial fractionation line

Table 1 Mean isotopic abundance ratios in the solar wind from spaceborne sensors

Volatile isotopes			Refractory isotopes		
Ratio	Spacecraft data	Apollo SWC/ meteorites	Ratio	Solar wind	Meteoritic values
$^{3}He/^{4}He^{(s)}$	0.00041 ± 0.000025[1)]	0.000142[2)]	$^{25}Mg/^{24}Mg$	0.1260 ± 0.0014[3)]	0.12658[2)]
$^{3}He/^{4}He^{(f)}$	0.00033 ± 0.000027[1)]	0.000142[2)]	$^{26}Mg/^{24}Mg$	0.1380 ± 0.0031[3)]	0.13947[2)]
$^{15}N/^{14}N$	≤ 0.005[4)]	0.0023(3)[5)]	$^{29}Si/^{28}Si$	0.05012 ± 0.00072[3)]	0.050634[2)]
$^{17}O/^{16}O$	≤ 0.0005[4)]	0.00038[2)]	$^{30}Si/^{28}Si$	0.03344 ± 0.00024[3)]	0.033612[2)]
$^{18}O/^{16}O$	≤ 0.002[4,6)]	0.0020[2)]	$^{42}Ca/^{40}Ca$	0.00657 ± 0.00017[3)]	0.006621[2)]
$^{21}Ne/^{20}Ne$	0.0023 ± 0.0006[3)]	0.0024(3)[7)]	$^{44}Ca/^{40}Ca$	0.0209 ± 0.0011[3)]	0.021208[2)]
$^{22}Ne/^{20}Ne$	0.0728 ± 0.0013[3)]	0.0726(3)[7)]	$^{54}Fe/^{56}Fe$	0.068 ± 0.004[9)]	0.06327[2)]
$^{38}Ar/^{36}Ar$	0.183 ± 0.018[8)]	0.1880[2)]	$^{57}Fe/^{56}Fe$	0.025 ± 0.005[9)]	0.02339[2)]

1) Gloeckler and Geiss (1998); 2) Anders and Grevesse (1989); 3) Kallenbach (2000; 2001); 4) this work; 5) Owen et al. (2001); 6) Collier et al. (1998), Wimmer-Schweingruber et al. (2001); 7) mean of solar wind ratios from Apollo SWC (Geiss et al. 1972) and from Palma et al. (2002); 8) Weygand et al. (2001); 9) Ipavich et al. (2001); (f): 'fast' solar wind; (s): 'slow' solar wind

It will be the great challenge of the Genesis team to deliver more precise results. A future analysis of the full measurement period of MTOF onboard SOHO of more than ten years may yield results with a higher precision due to better counting statistics. Principal difficulties will remain because of the interference of doubly charged Si and S isotopes in the

time-of-flight spectra. However, when Genesis data are available, a re-evaluation of MTOF data may still be worthwhile.

Appendix

As mentioned in Sect. 2, the main difficulty in determining the abundance of the rare ^{15}N isotopes in MTOF data comes from the interference of $^{30}Si^{++}$ with $^{15}N^{+}$ in the time-of-flight spectra. Additionally, the tail of the peak measured for the more abundant $^{14}N^{+}\&^{28}Si^{++}$ needs to be subtracted from the peaks of the less abundant $^{29}Si^{++}$ and $^{15}N^{+}\&^{30}Si^{++}$ that lie on top of it. This subtraction is very critical and presumably the main source of possible systematic uncertainties. However, the technique presented here reproduces the correct $^{29}Si^{++}$ and $^{30}Si^{++}$ count numbers that has been derived independently from the determination of the FIP-fractionation in the solar wind during the measurement period.

In K98 the line shapes have been described by analytical functions. These functions may not be correct in the far ends of the tails of the peaks. In this analysis, we have verified that the various peaks in the MTOF spectra can be described by a series of ratios $R_{\mathrm{down};i} = \Delta N_{i+1}/\Delta N_i$, $\Delta N_i = N_{i+1} - N_i$, where N_i are the counts in channel i. The ratios typically range from $R_{\mathrm{down};i} \approx 0.5$ at a few channels above the peak center to $R_{\mathrm{down};i} \approx 0.8$ in the far end of the peak. This kind of numerical fit has most precisely been applied to the $^{16}O^{+}$ peak which is assumed to be similar to the $^{14}N^{+}\&^{28}Si^{++}$ peak. This is justified because all peaks in the MTOF data have a similar form and in particular because of the fact that the mass-per-charge ratios of $^{16}O^{+}$, $^{14}N^{+}$, and $^{28}Si^{++}$ are similar. In the following, we assume the technique being precise. However, in the final result we include the difference to the result obtained with the original method in K98 as an upper limit for a possible systematic error.

Data Analysis for the Nitrogen Isotopes

Determination of the $^{29}Si^{++}$ and $^{15}N^{+}\&^{30}Si^{++}$ Counts from Line Shape Analysis

As stated earlier, we assume that the shape of the $^{14}N^{+}\&^{28}Si^{++}$ peak extending to the $^{29}Si^{++}$ and $^{15}N^{+}\&^{30}Si^{++}$ mass range and the shape at the right-hand side of the $^{16}O^{+}$ peak are described by identical ratios $R_{\mathrm{down};i} = \Delta N_{i+1}/\Delta N_i$, $\Delta N_i = N_{i+1} - N_i$, where N_i are the counts in channel i. This yields the black line in Fig. 2. The actual counts for the different channels are listed in Table 2.

Beyond channel 25 the sequence includes $^{17}O^{+}$ for channels 58 through 63. However, the average number $R_{\mathrm{down}} = 0.80 \pm 0.08$ reproduces the black line below the $^{17}O^{+}$ peak. This sequence converges to the background level of 30,000 apparent from the convergence of the right wing of the $^{16}O^{+}$ peak. This background is also used in Table 2.

The background level of 30,000 defines a mean R_{up} number for channels 26 through 31. Extrapolating the left-hand side of $^{16}O^{+}$ leads to a total difference of $(52{,}289 - 42{,}997) \times R_{\mathrm{up}}/(1 - R_{\mathrm{up}}) = 42{,}997 - 30{,}000 = 12{,}997$ and thus $R_{\mathrm{up}} \approx 0.583$. From that the $^{16}O^{+}$ "wing" below $^{15}N^{+}\&^{30}Si^{++}$ is determined. In our view, there is no better explicit way to estimate the line shapes below the $^{15}N^{+}\&^{30}Si^{++}$ counts. In particular, the "electronic ringing" peak hampers the analysis of the line shape. "Ringing" is an instrumental effect that occurs in the time-of-flight electronics. It means that a fraction of 0.12 of TOF measurements for any ion species is systematically shifted by a fixed channel number to shorter times. This is best visible at the left-hand side of the $^{16}O^{+}$ peak but also to the left of the $^{14}N^{+}/^{28}Si^{++}$

Table 2 Overview of data analysis

Ch #	Counts	R_{down}*	$^{14}N^{+}$ &$^{28}Si^{++}$	R_{up}*	$^{16}O^{+}$	$^{14}N^{+}$& $^{28}Si^{++}$ +$^{16}O^{+}$ a)
17	102,137	0.579	102,137	–	–	102,137
18	75,731	0.490	75,731	–	–	75,731
19	63,007	0.605	59,769	–	–	59,769
20	55,757	0.595	50,271	–	–	50,271
21	52,034	0.593	44,639	–	–	44,639
22	47,966	0.630	41,094	–	–	41,094
23	42,615	0.670	38,718	–	–	38,718
24	37,713	0.710	37,032	–	–	37,032
25	35,757	0.759	35,757	–	–	35,757
26	36,851	0.800	34,612	0.583	30,517	35,129
27	38,566	0.800	33,696	0.583	30,882	34,578
28	38,816	0.800	32,963	0.583	31,508	34,471
29	40,124	0.800	32,377	0.583	32,581	34,958
30	40,972	0.800	31,908	0.583	34,422	36,330
31	41,085	0.800	31,533	0.583	37,580	39,113
32	42,997	–	–	0.401	42,997	42,997
33	52,289	–	–	0.645	52,289	52,289

R_{down} belongs to the $^{14}N^{+}$&$^{28}Si^{++}$ peak, R_{up} to the $^{16}O^{+}$ peak

a) Sum of $^{14}N^{+}$&$^{28}Si^{++}$ and $^{16}O^{+}$ based on a background level of 30,000 in the channels between the $^{14}N^{+}$&$^{28}Si^{++}$ and $^{16}O^{+}$ lines

*Averaged over four channels of the $^{16}O^{+}$ peak to reduce statistical variations and multiplied by a factor 1.0425 in order to connect the count number of channel 18 to the count number of channel 25

peak. It has been checked that the used line shapes—that is, the numbers $R_{up/down}$—are similar to the numbers found for instance at the $^{28}Si^{+}$ peak and the $^{56}Fe^{+}$ peak. The uncertainty of the numbers $R_{up/down}$ is typically 15%.

The procedure yields 27,569 counts for $^{29}Si^{++}$. The background below $^{29}Si^{++}$ is 271,523 counts and yields an uncertainty of 521 counts. For $^{15}N^{+}$&$^{30}Si^{++}$ we get 21,835 counts with a background of 214,579; that is, with an uncertainty of 463 counts. We now have to correct the $^{29}Si^{++}$ by $0.12 \times 21{,}835 \approx 2{,}620$ counts which spill over from the $^{15}N^{+}$&$^{30}Si^{++}$ peak to the $^{29}Si^{++}$ peak; that is, $^{29}Si^{++} = 24{,}949 \pm 521$. The $^{30}Si/^{29}Si$ ratio in the solar wind is about 0.68 ± 0.03 (Kallenbach 2003), consistent with the meteoritic value (Anders and Grevesse 1989), and $^{30}Si^{++}$ is detected more efficiently than $^{29}Si^{++}$ by a factor 1.04. Therefore, we must multiply $^{29}Si^{++}$ by a factor 0.7072 to get the number $^{30}Si^{++} = 17{,}644$. This method finally yields $^{15}N^{+} = 4{,}191$.

$^{29}Si^{++}$ *Counts from Determination of the FIP Fractionation*

We have verified the Si counts by determining the FIP fractionation and thus the elemental abundance ratio Si/N in the solar wind during the measurement time period. In the slow solar wind Si can be enriched by the FIP fractionation process up to a factor of 3 to 4 with respect to its photospheric abundance, however, from Fig. 3 it follows that MTOF *counts* an average enrichment of Mg by the FIP effect of only about 1.4. From the photospheric

Table 3 Data analysis: Oxygen isotopes

Ch #	Counts	R_{down}	$^{16}O^{+}$	Ch #	Counts
67	33,314			78	29,688
68	31,431			79	29,601
69	30,867	0.8	30,867	80	29,090
70	31,409	0.8	31,409	81	29,848
71	32,180	0.8	32,180	82	31,491
72	33,262	0.8	33,262	83	32,091
73	35,603	0.8	35,603	84	30,792
74	38,125	0.8	38,125	85	30,222
75	36,787	0.8	36,787	86	30,300
76	30,799	0.8	30,799	87	30,077
77	28,850	0.8	28,850	88	29,642

ratio $^{28}Si/^{14}N = 0.296$ (Anders and Grevesse 1989) it follows that $^{28}Si/^{14}N \approx 0.415$ in the solar wind during the measurement period. A detailed analysis of calibrated instrument functions (Gonin et al. 1994; Kallenbach et al. 1995) gives a higher detection efficiency of $^{14}N^{+}$ than for $^{28}Si^{+}$ by a factor 1.18. Therefore, we have a fraction of 26% of the 1,635,988 counts within 6 channels around the peak center of $^{14}N^{+}\&^{28}Si^{++}$ as $^{28}Si^{++}$ counts; that is, $^{28}Si^{++} \approx 425{,}357$. The $^{28}Si/^{29}Si$ ratio is about 19.7 (Anders and Grevesse 1989), as confirmed by MTOF measurements (Kallenbach 2003), and $^{29}Si^{++}$ is detected more efficiently than $^{28}Si^{++}$ by a factor 1.07 (K98). This yields $^{29}Si^{++} \approx 23{,}103$. Correcting the 2,620 counts of spill-over from $^{15}N^{+}\&^{30}Si^{++}$ through "ringing" this yields $^{29}Si^{++} \approx 20{,}483$. Comparison to $^{29}Si^{++} \approx 24{,}949$ suggests that the line shape method may lead to a background level that gives 4,516 counts more for $^{29}Si^{++}$. This would mean that the line shape method also could overestimate the $^{15}N^{+}\&^{30}Si^{++}$ counts by as much as 4,516 counts; that is, $^{15}N^{+}\&^{30}Si^{++}$ could be as low as 17,319. Multiplying $^{29}Si^{++}$ by 0.7072 as above, we get $^{30}Si^{++} \approx 14{,}486$. The method finally yields $^{15}N^{+} = 3{,}433$.

Determination of $^{15}N/^{14}N$

With this information we now have to determine a ratio $^{15}N/^{14}N$. The two methods above yield an average value $^{15}N^{+} \approx 3{,}812 \pm 536$. However, we have to add the statistical uncertainty introduced by the background of roughly 271,523 below $^{29}Si^{++}$ and 214,579 below $^{15}N^{+}\&^{30}Si^{++}$. The total statistical uncertainty is thus about 591 counts. This yields $^{15}N^{+} \approx 3{,}812 \pm 798$.

The number of $^{14}N^{+}$ counts is $1{,}635{,}988 - 425{,}357 = 1{,}210{,}631$. Considering the fact that $^{15}N^{+}$ is detected more efficiently than $^{14}N^{+}$ by a factor 1.055 (K98), this yields $^{14}N/^{15}N \approx 320$ or $^{15}N/^{14}N \approx (3.1 \pm 0.7) \times 10^{-3}$. This is marginally consistent with the value $^{15}N/^{14}N \approx (2.3 \pm 0.3) \times 10^{-3}$ measured with the GPMS in Jupiter's atmosphere (Owen et al. 2001), but also consistent with the terrestrial ratio. Considering the uncertainty of the analysis of data with such large background, we basically repeat the result of Kallenbach (2003) that $^{14}N/^{15}N > 200$ in the solar wind.

Data Analysis for the Oxygen Isotopes

The CELIAS/MTOF data give about 7,158,000 counts within seven channels for $^{16}O^{+}$ and about $31{,}400 \pm 500$ counts for $^{18}O^{+}$ & $^{36}Ar^{++}$ (Table 3). The contribution of $^{36}Ar^{++}$ can be

estimated from the $^{38}Ar^{++}$ peak in which the contribution of $^{57}Fe^{+++}$ is negligible. Taking a background of $29,803 \pm 394$ from channels 78–80 and 85–88, that is, for a maximum background of 30,197 we get at least 3,911 counts for $^{38}Ar^{++}$. With $^{36}Ar/^{38}Ar$ of about 5.3 in the solar wind and a more efficient detection of $^{38}Ar^{++}$ by about 20% as a typical maximum number for MTOF, we find at most about 14,600 counts of $^{18}O^{+}$ and thus $^{16}O/^{18}O \geq 500$. In a similar way, we find $^{16}O/^{17}O \geq 2{,}000$ if there is no contribution of $^{34}S^{++}$ to the peak of $^{17}O^{+}$. However, the meteoritic $^{34}S/^{17}O$ ratio is about 2.4 and the ratio of the detection efficiencies of $^{34}S^{++}$ and $^{17}O^{+}$ is about 0.4 (Kallenbach et al. 1995) so that $^{34}S^{++}/^{17}O^{+}$ may be of order unity in the MTOF spectrum. Therefore, a depletion of ^{17}O in the solar wind with respect to terrestrial ^{17}O does not seem unlikely.

References

M.M. Abbas et al., Astrophys. J. **602**, 1063 (2004)
E. Anders, N. Grevesse, Geochim. Cosmochim. Acta **53**, 197 (1989)
R.N. Clayton, LPSI 33 # 1326, 2002
M.R. Collier et al., J. Geophys. Res. **103**, 7 (1998)
T. Fouchet et al., Icarus **172**, 50 (2004)
J. Geiss et al., NASA SP **315**, 14.1 (1972)
G. Gloeckler, J. Geiss, Space Sci. Rev. **84**, 275 (1998)
M. Gonin et al., NIM B **94**, 15 (1994)
K. Hashizume et al., 31st Lun. Planet. Sci. Conf., #1565, 2000
K. Hashizume, M. Chaussidon, Nature **434**, 619 (2005)
E. Herbst, Space Sci. Rev. **106**, 293 (2003)
F.M. Ipavich et al., AIP CP **598**, 121 (2001)
E. Jehin et al., Astrophys. J. **613**, L161 (2004)
D.C. Jewitt et al., Science **278**, 90 (1997)
R. Kallenbach et al., NIM B **103**, 111 (1995)
R. Kallenbach et al., ESA SP **415**, 33 (1998a)
R. Kallenbach et al., Astrophys. J. **507**, L185 (1998b)
R. Kallenbach, *Isotopic Composition of the Solar Wind* (University of Bern, Bern, 2000)
R. Kallenbach, AIP CP **598**, 113 (2001)
R. Kallenbach, Space Sci. Rev. **106**, 305–316 (2003)
H. Lammer, S.J. Bauer, Space Sci. Rev. **106**, 281 (2003)
M.-C. Liang et al., Astrophys. J. **657**, L117 (2007)
B. Marty et al., Space Sci. Rev. **106**, 175 (2003)
S. Messenger et al., Space Sci. Rev. **106**, 155 (2003)
H.B. Niemann et al., Nature **438**, 779 (2005)
T. Owen et al., Astrophys. J. **553**, L77 (2001)
R.L. Palma et al., Geochim. Cosmochim. Acta **66**, 2929 (2002)
M.H. Thiemens, J.E. Heidenreich III, Science **219**, 1073 (1983)
R. von Steiger, J. Geiss, Astron. Astrophys. **225**, 222–238 (1989)
J.M. Weygand et al., Geochim. Cosmochim. Acta **65**, 4589 (2001)
R. Wieler et al., EPSL **167**, 47 (1999)
R.F. Wimmer-Schweingruber et al., Geophys. Res. Lett. **28**, 2763 (2001)